An investigation into the optical properties of quantum dots and other materials using a homemade spectrometer and self-written software

By Jack Lipman

Abstract

Analysis of a range of light sources and luminescent materials (including filament lamps, LEDs, lasers, elemental discharge lamps, fluorescent molecules and quantum dots) has been carried out using a homemade spectrometer based on a simple webcam and diffraction grating. The spectrometer has an optical range of 350nm to 770nm and a spectral resolution of 19nm (FWHM). By creating bespoke software, the spectra produced from these sources are available in near real-time, and are used to investigate the theory behind the materials involved. Quantum dots are given particular focus due to their unique optical properties which mimic those of individual atoms and can be described by a simple quantum mechanical model. By analysing the emission spectrum of a sample of graphene quantum dots an estimate of the effective mass of an electron within these structures was derived to be $1.32 \pm 0.03 \times 10^{-32}$kg which corresponds to approximately 1.4% the rest mass of an electron. A significant finding was a dual peak in the emission spectrum of the sample of quantum dots. While the cause is unknown and warrants further investigation, it suggests the presence of two distinct sizes of graphene quantum dots which differ in size by approximately 0.3nm, corresponding to just 1 or 2 rows of carbon atoms in the lattice.

Introduction

Spectroscopy is the study of the interaction between matter and electromagnetic radiation. It is performed by analysing the wavelength and intensity of the radiation which is absorbed or emitted during the interaction. Spectroscopy is generally carried out by splitting the light emitted from a substance into its constituent wavelengths (known as a spectrum), historically using glass prisms.[i,ii] In modern practice, a diffraction grating is used. Interference between light spreading out from the closely spaced slits of the diffraction grating leads to constructive maxima at fixed angles from a central maximum according to the grating equation.

$$d \sin \theta = n\lambda$$

Spectroscopy can be used to determine the chemical composition and physical properties of various materials, ranging from laboratory samples to distant extraterrestrial objects such as stars and galaxies.[iii] Spectroscopy can also be used to investigate phenomena such as fluorescence in various materials.[iv]

Spectroscopy can be an expensive process requiring high levels of precision, but it is possible to investigate and illustrate many of its uses using simple principles and apparatus. This paper will present measurements and analysis made using a homemade spectrometer and self-written software.

Description of Spectrometer

Apparatus

A cross-sectional diagram of the homemade spectrometer is illustrated in Figure 1 and the final apparatus is pictured in Figure 2.

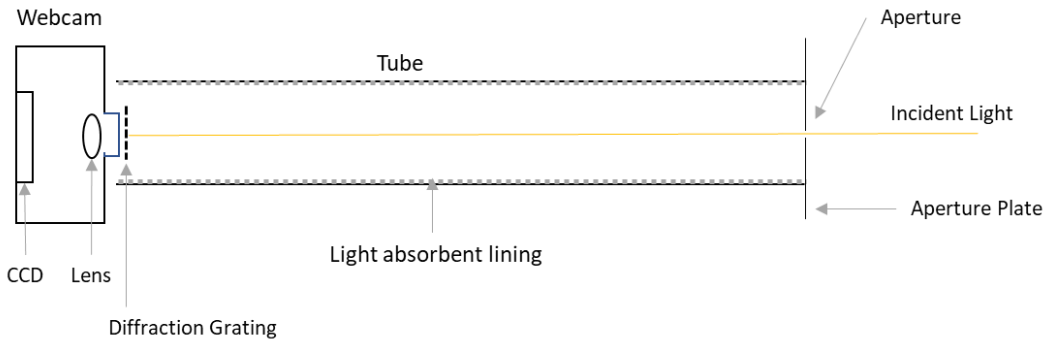

Figure 1 - Diagram of the spectrometer

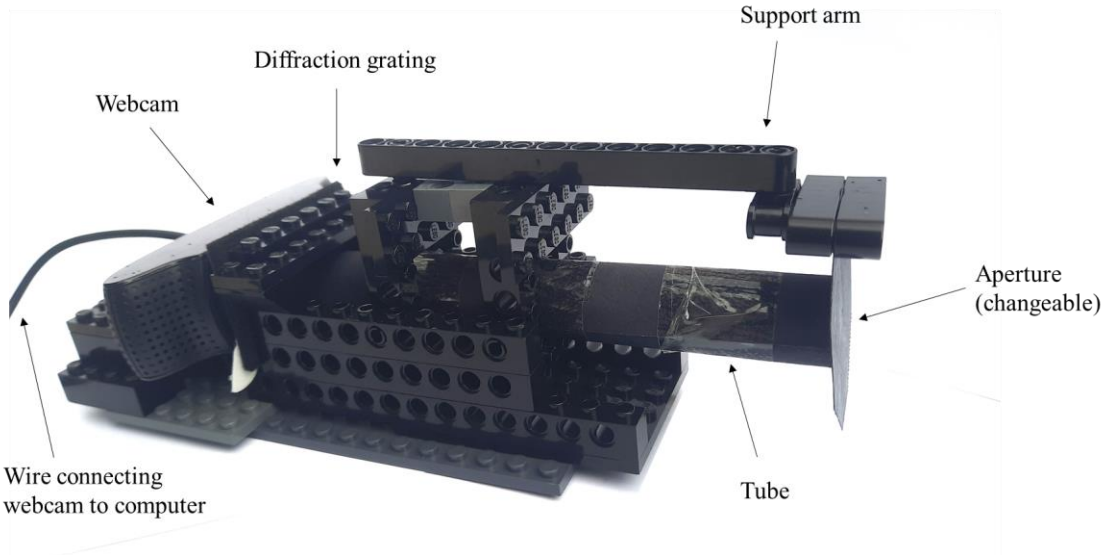

Figure 2 - Image of Spectrometer

The spectrometer consists of a transmission diffraction grating fixed directly onto the lens of a webcam (*Xiaomi IMILAB CMSXJ22A 1080P Full HD).* These are mounted behind a long tube that connects to the aperture plate which contains a small circular aperture through which light enters the apparatus. The aperture plate is easily replaceable, allowing for different sizes and shapes of aperture to be used. The sealed and light absorbent setup minimises light ingress other than through the entrance aperture in order to maximise the contrast of the diffraction spectrum.

Incident light is split by the diffraction grating onto the lens which focuses the light onto the charge-coupled device (CCD) detector of the webcam. In this way, the constituent wavelengths of the incident light arrive at different positions on the CCD to create a spectrum. The webcam is connected to a computer for image processing and analysis.

Image Processing and Calibration

An example of a raw image taken from the webcam is illustrated in Figure 3, showing the central maximum at the centre and first order spectra on either side.

Figure 3 – Sample Output Image

Image processing is performed by self-written software (Appendix A) which converts the raw webcam image into a graph of relative light intensity against wavelength in several stages.

First, the image is converted into arrays of pixel number and intensity. Next, a zero point is established using the intensity weighted average position of the central maximum peak[1], allowing the distance in pixels from any point to the centre of the spectrum to be calculated. An example of a normalised spectrum is shown in Figure 4.

[1] This dynamic method of establishing the zero point is an important feature which improves reliability of the calibration since it removes the need for precisely aligned incident light. This is also a superior estimator of the centre compared to using the maximum intensity value, especially for saturated maxima.

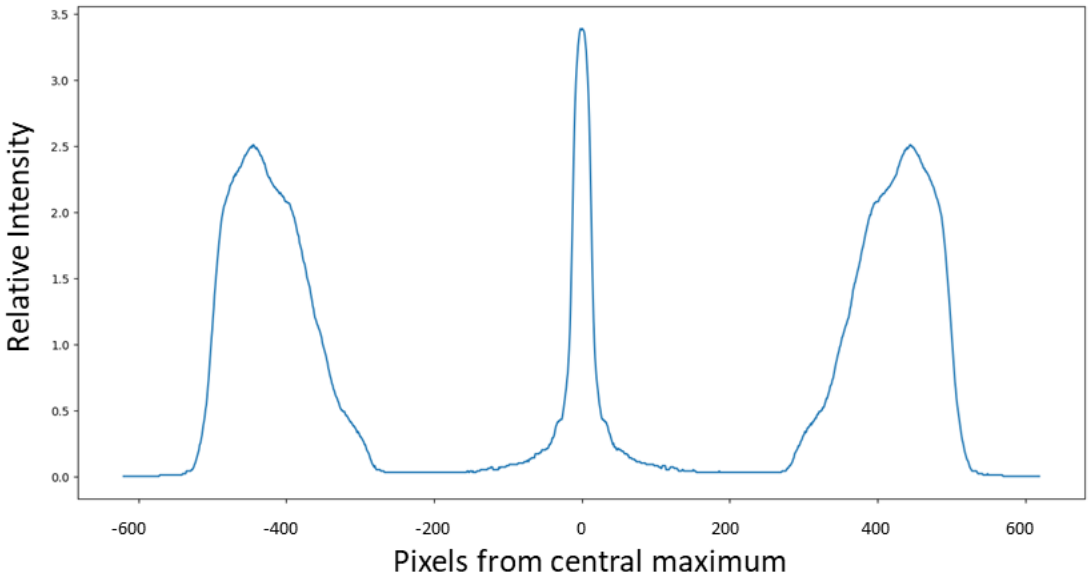

Figure 4 – Normalised output graph

The spectrometer is calibrated using lasers due to their narrow emission profiles. Four lasers with wavelengths of 405nm, 450nm, 532nm and 650nm are used. The average distance in pixels of each laser spectral peak (one on each side of the central maximum) to the zero point is calculated. These values are then plotted against their corresponding wavelengths and are fitted to establish a calibration function as illustrated in Figure 5.

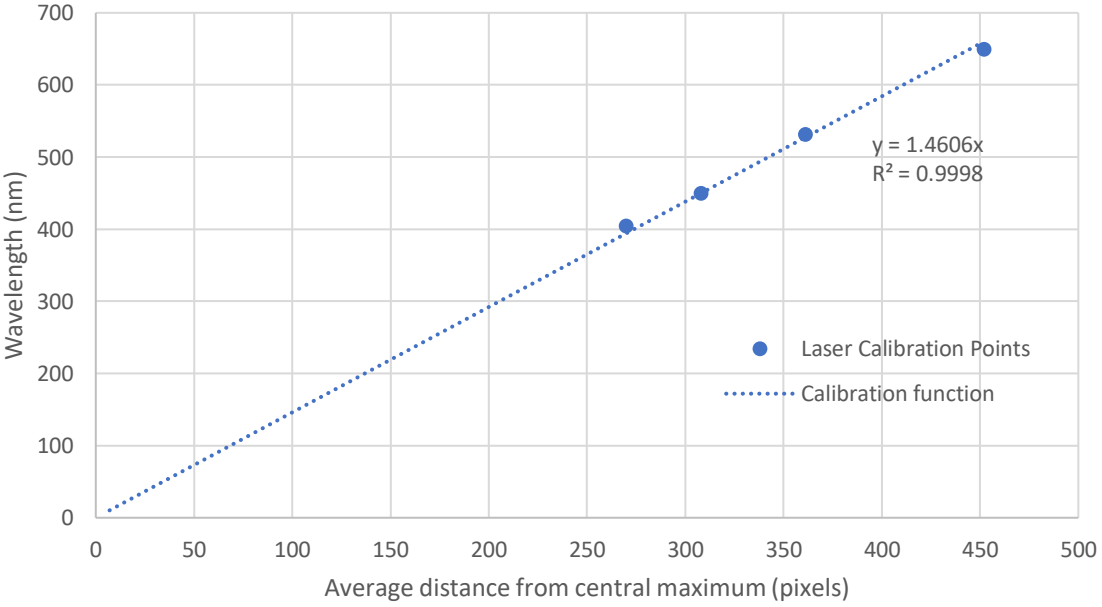

Figure 5 – Wavelength vs Average distance from central maximum

This is an obvious linear relationship, and there is no requirement to use any higher order polynomial fit. This linearity is likely due to the focusing of light from the lens as well as the angles involved being small enough for $\sin\theta \approx \theta$.

This calibration enables the software to convert raw images taken from the webcam directly into graphs of relative intensity against wavelength, rather than pixel number, allowing spectroscopy to be carried out using the apparatus.

Optical range

In order to determine the optical range of the spectrometer, two sources were used to cover a broad range of wavelengths: a filament lamp extending into the red range, and a UV lamp covering the blue/purple range. The spectra from these sources are illustrated in Figure 6, demonstrating that the range of the instrument is from approximately 350nm to 770nm. This extends into both the infra-red and ultraviolet regions of the spectrum beyond the limits classically thought to be visible to the human eye[v], but within the range established by more recent research.[vi]

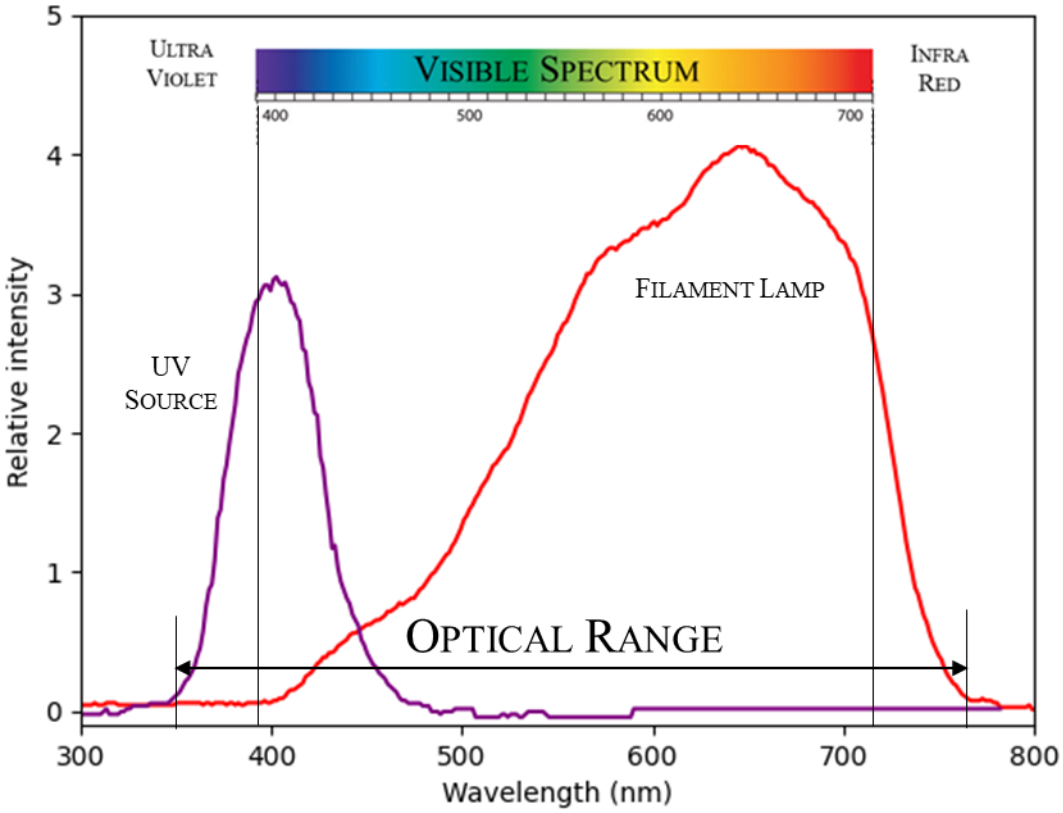

Figure 6 - Spectra of Filament Lamp and UV source to demonstrate the optical range of the spectrometer

Spectral Resolution

We can investigate the spectral resolution of the spectrometer by analysing the spectrum of a narrow band light source such as a laser. The spectral peak from a green frequency-doubled Nd:YAG[vii] laser with wavelength 532 ± 10 nm is illustrated in Figure 7 superimposed on the spectrum of the filament lamp from above, highlighting the difference in wavelength range.

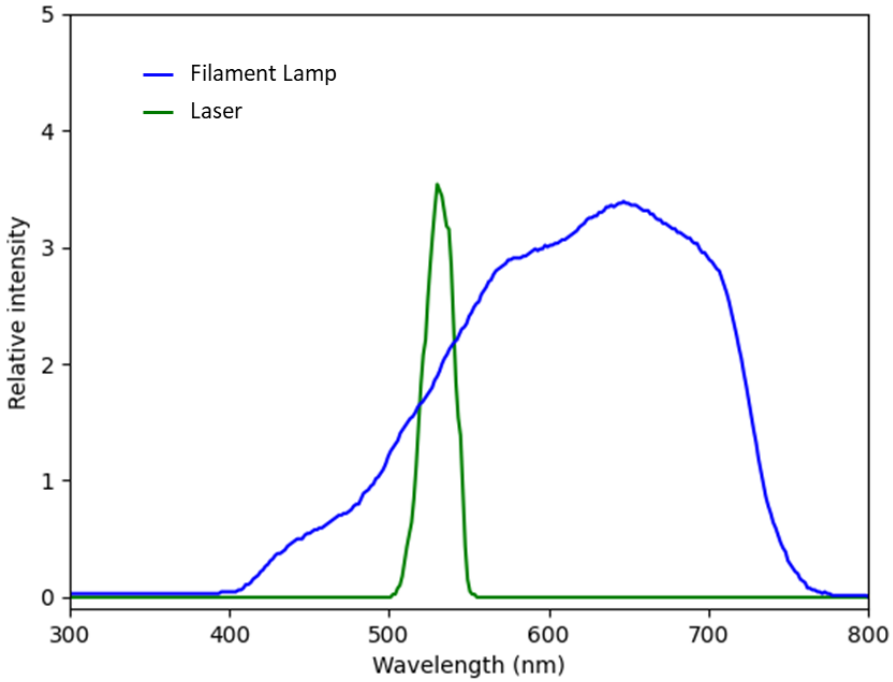

Figure 7 - Spectra of filament lamp and laser

The laser spectrum is illustrated on an expanded scale in Figure 8, showing a full width at half maximum (FWHM) of 19nm. This corresponds to a half width of 9.5nm which is equivalent to approximately 6 pixels.

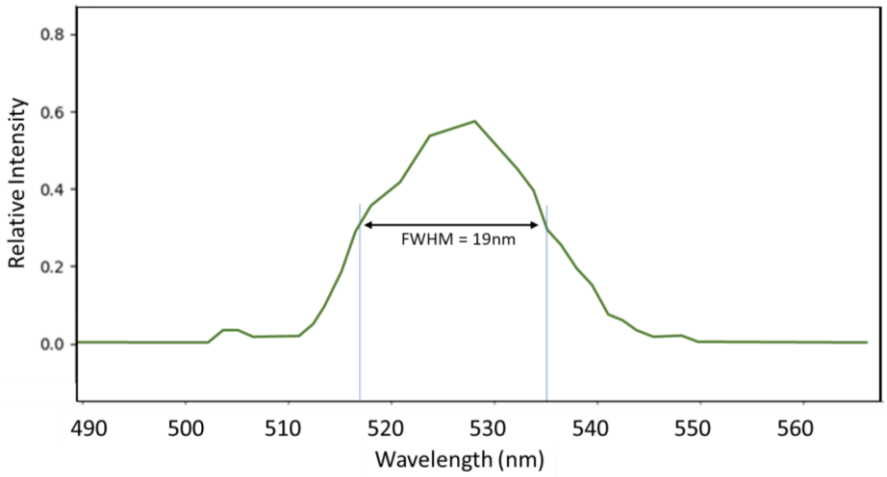

Figure 8 - FWHM of laser spectrum to demonstrate the spectral resolution of the spectrometer

Investigation 1: Elemental Gases

All elements have unique sets of atomic orbitals since they have different electronic configurations. Since the emission and absorbance of electromagnetic radiation is determined by the difference in energy between energy levels, each element has a unique set of emission and absorption spectra. This allows different elements to be distinguished by the spectra they produce.[viii]

Figure 9 shows emission spectra taken of three different elemental discharge lamps, illustrating their unique spectral peaks which can be used for identification.

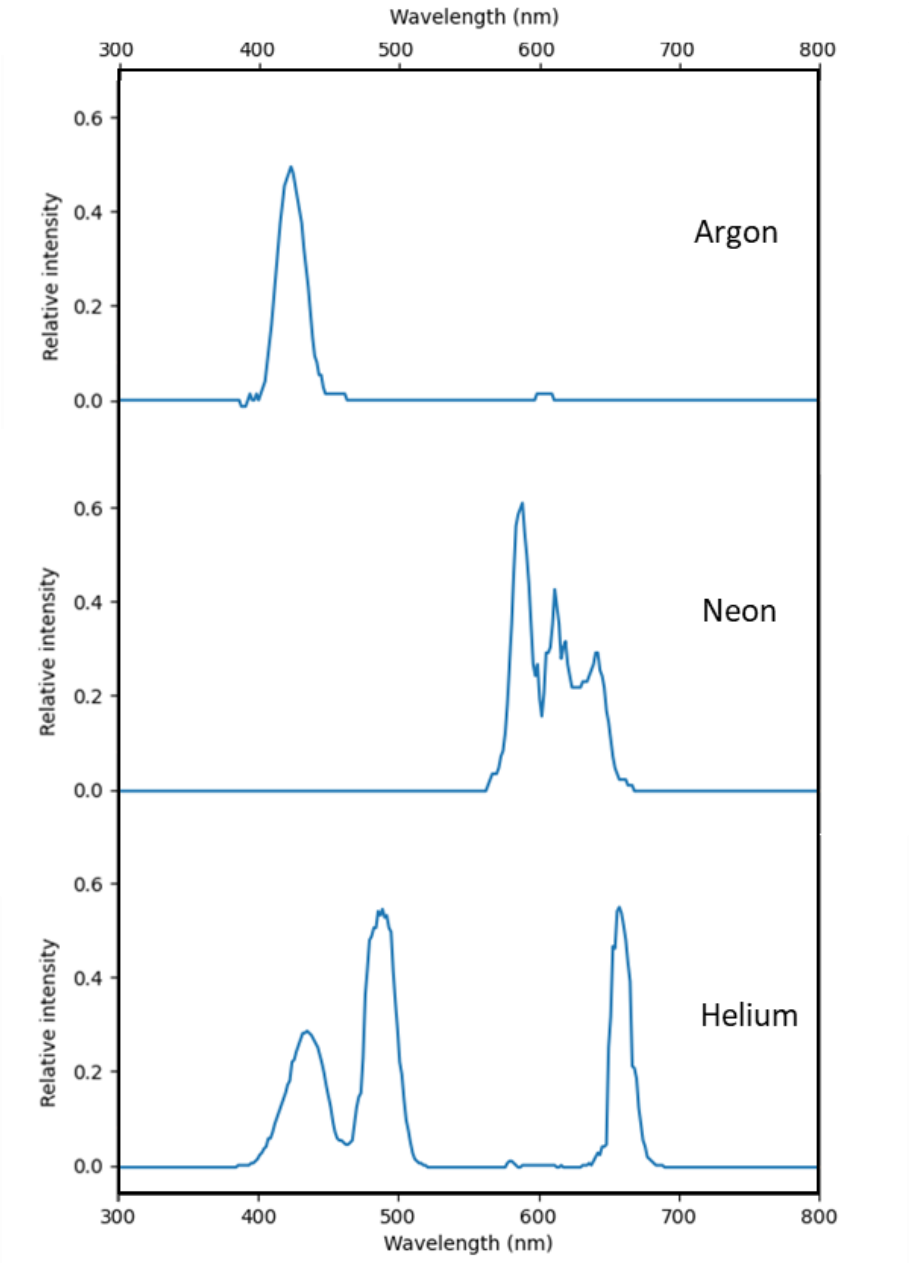

Figure 9 - Spectra of several elemental discharge lamps

Due to the unique absorption and emission spectra of elements, spectroscopy can be used to determine the chemical composition of unknown light sources. For example, Figure 10 illustrates an emission spectrum taken from a streetlamp of unknown composition.

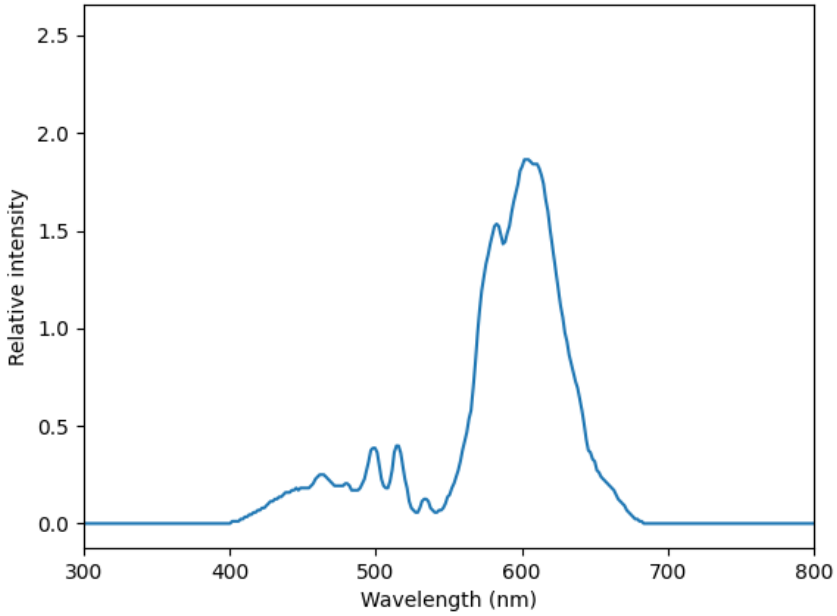

Figure 10 - Spectrum of a streetlamp

The most intense spectral peak is at approximately 580nm to 620nm, giving rise to the orange/yellow hue of the light emitted from the streetlamp. This corresponds with the sodium D-lines (an intense doublet with wavelengths of 589.0 and 589.6nm)[ix], suggesting that streetlamp is primarily composed from sodium.

Analysis of spectra in this way is commonly used in laboratories to determine the composition of materials.[x] Using the same principles, spectroscopy is also used for the analysis of more complex systems, a particularly interesting example of which is investigating distant stars and galaxies.[xi] By observing the spectrum of a distant object, the position and intensity of the emission or absorption spectral lines can be measured to determine which elements are present, and their relative abundances.[xii,xiii] There are added layers of complexity due to redshift, extreme temperatures and the possibility of multiple sources, which inform astronomers of the conditions of the light source, intervening matter and distance on a universal scale. [xiv]

One of the most notable examples of this technique was the discovery of helium through analysis of the spectra produced by solar prominences in the Sun. In these spectra, a yellow spectral line was observed which did not correspond to the spectra of any of the known elements at the time in 1868.[xv] This result provided evidence for the existence of a new element, which was later confirmed by experiments in 1895 which detected helium produced from uranium ore.[xvi]

Investigation 2: Light sources

In this section spectroscopy is used to investigate a number of light sources in order to highlight the different physical processes behind their functions.

Lasers

Laser stands for "Light Amplification by Stimulated Emission of Radiation".[xvii] Lasers function by amplifying a specific wavelength of coherent electromagnetic radiation, producing a very narrow and monochromatic beam of coherent light. This is demonstrated by the spectrum illustrated earlier in Figure 8, where the FWHM was 19nm. In reality, the emission spectrum is much narrower, but our measurements are limited by the resolution of the spectrometer.

Light Emitting Diodes

An LED (Light Emitting Diode) is a semiconductor which emits light when a current is applied.[xviii] The current supplies energy to promote electrons from the valence band of the semiconductor to the conduction band. When these conduction electrons recombine with electron holes in the valence band, energy equal to the band gap of the semiconductor is emitted as electromagnetic radiation through a process known as electroluminescence. As a result, the wavelength of light emitted is determined by the band gap of the semiconductor.[xix] The spectrum obtained from a red LED is illustrated in Figure 11. The wavelengths emitted by LEDs are not as specific as in the light emitted by lasers, as can be seen from the FWHM of 44nm. LED light is also not coherent and, so cannot reach the same level of brightness as laser light.[xx]

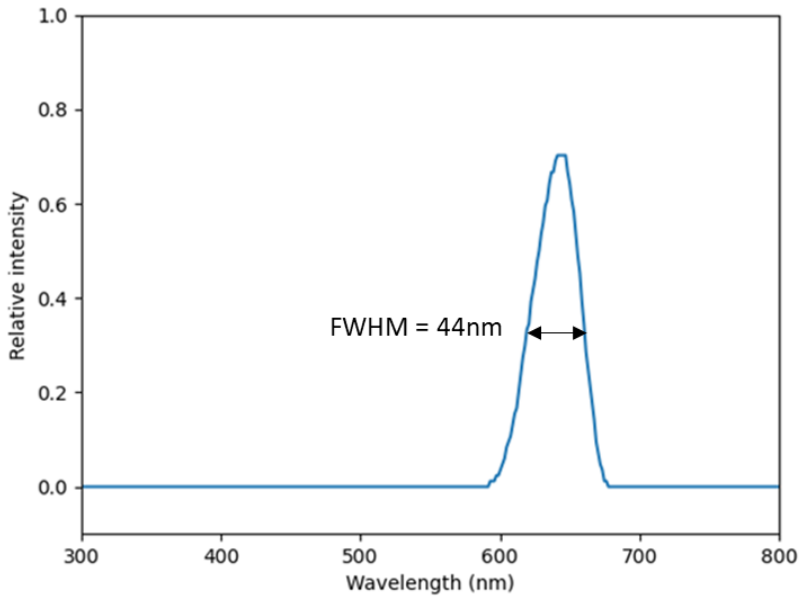

Figure 11 - Spectrum of a red LED

Domestic LED lights generally produce white light using three LEDs which correspond to red, green and blue emission wavelengths.[xxi] The spectrum obtained from a white LED light is illustrated in Figure 12, showing three emission peaks each corresponding to one of the constituent LEDs.

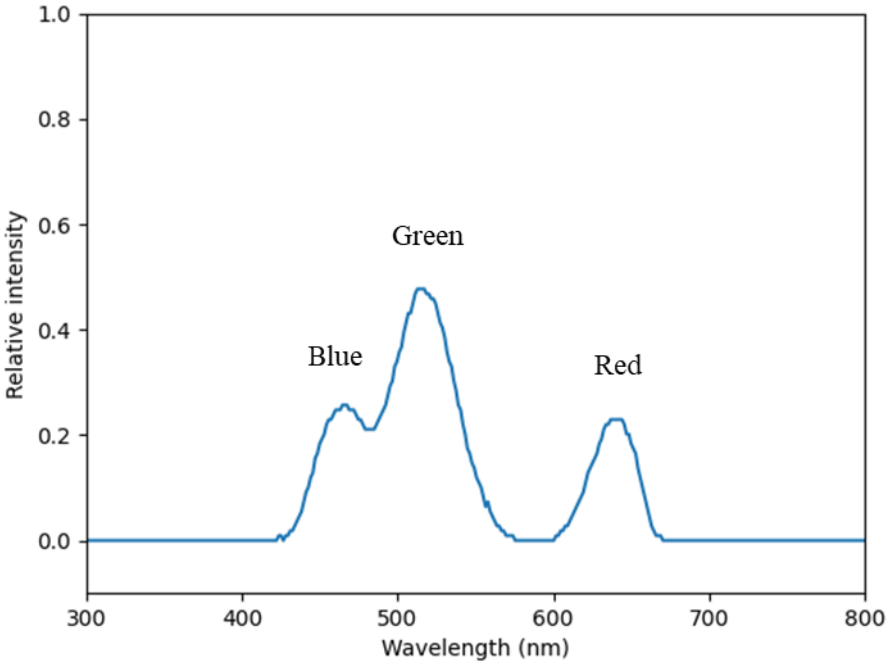

Figure 12 - Spectrum of white LED light showing the three constituent LEDs

LEDs have numerous advantages over other sources of light such as incandescent bulbs, including a lower power consumption, higher efficiency, longer lifetime, and smaller physical size.[xxii] The current through each semiconductor can also be varied in order to change the intensity of their emitted light, allowing many different colours to be produced.[xxi] This is demonstrated in Figure 13, which illustrates the spectra obtained from various colours of LEDs.

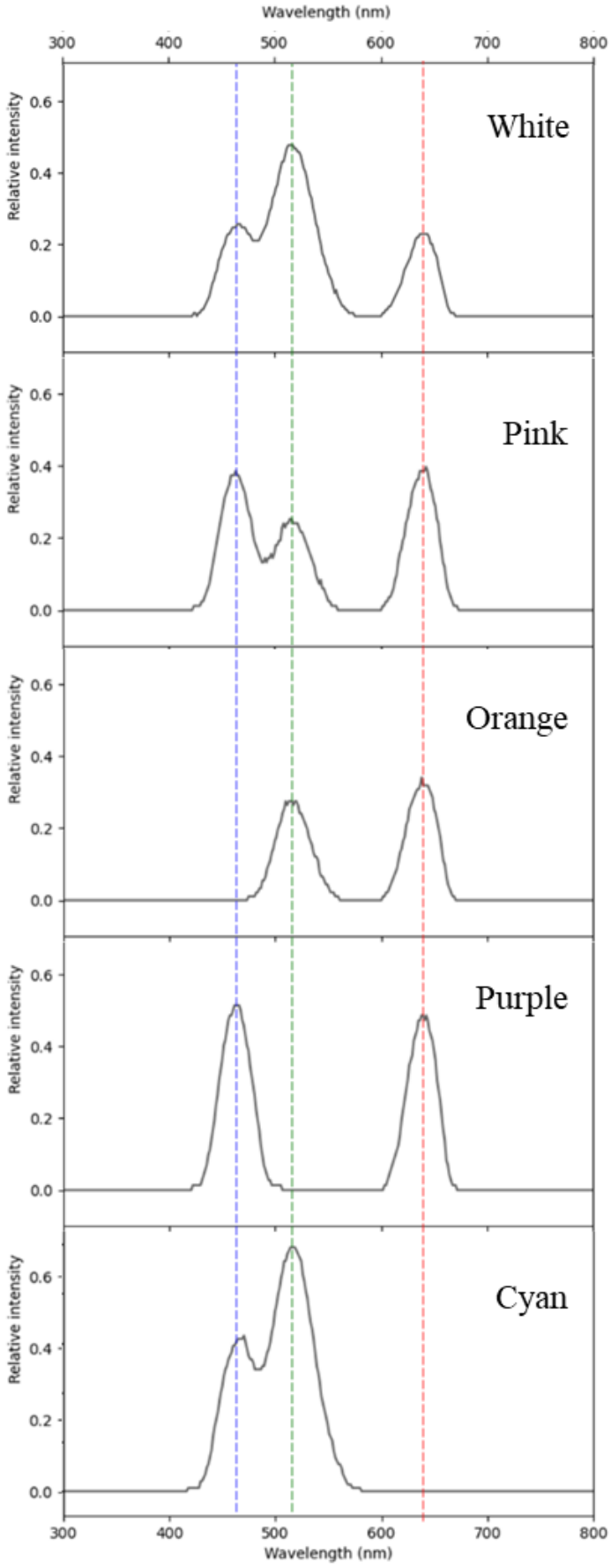

Figure 13 - Spectra of various colours of LEDs

Filament lamps

Filament lamps contain a wire filament which is heated to a high temperature, causing it to glow and emit light in a process known as incandescence. [xxiii] The filament is surrounded by an inert gas such as argon and is enclosed within a glass bulb, allowing the filament to reach high temperatures without becoming oxidised.[xxiv] The light emitted by a filament lamp is a continuous spectrum which closely resembles that emitted by a blackbody at the same temperature (a hypothetical perfect emitter and radiator of electromagnetic radiation)[xxv]. The characteristics of this radiation depend on the temperature of the body but not the nature of the body itself, as described by Planck's Law[xxvi] which gives spectral radiance as a function of the wavelength of the radiation emitted.

$$B_\lambda(\lambda, T) = \frac{2hc^2}{\lambda^5} \frac{1}{e^{\frac{hc}{\lambda k_B T}} - 1}$$

2

The spectrum obtained from a filament lamp is illustrated in Figure 14.

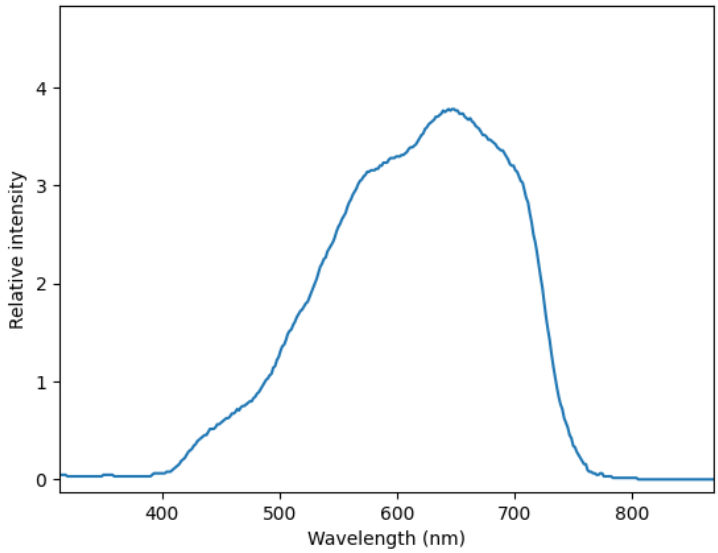

Figure 14 - Spectrum of a filament lamp

This spectrum is continuous across most of the wavelengths within the range that can be detected by the CCD. In theory, it would be possible to fit this graph using Planck's Law in order to determine the temperature of the filament. However, since we do not know the sensitivity of the CCD over this range of wavelengths, this is difficult to do in practice.

Investigation 3: Fluorescence

Fluorescence is a type of luminescence in which a material emits light after absorbing other electromagnetic radiation.[xxvii] Generally the emitted light has a lower energy than the absorbed radiation, and therefore has a longer wavelength.

Fluorescent molecules, also known as fluorophores, have many current uses including optical brightening agents for paper and textiles and chemical dyes for biological imaging and microscopy.[xxviii, xxix] In the following section the basic principles of fluorescence in molecular systems are explored, using the spectrometer to investigate examples of such molecules.

When incident radiation is absorbed by an electron in a fluorophore, the electron gains energy and is excited from its ground state to a higher energy state. The electron will generally lose some of its energy via vibrational relaxation before returning to its ground state. [xxx] This final transition is accompanied by the emission of a photon which generally has a lower energy than the absorbed photon due to a phenomenon known as Stokes shift.[xxxi] This occurs due to energy loss during the lifetime of the excited state caused by non-radiative vibrational relaxation, or the final state of the electron having higher energy than its initial state.

The ground state of most molecules is a singlet state, S_0, and fluorescence occurs most commonly during transitions between this state and the first singlet excited state of the molecule, S_1.

$$S_0 + h\nu_{excitation} \rightarrow S_1$$

$$S_1 \rightarrow S_0 + h\nu_{emission}$$

3

The mechanisms involved in fluorescence can be illustrated on a Jablonski diagram[xxxii] as depicted in Figure 15, which shows the energy states of the excited electron during the process.

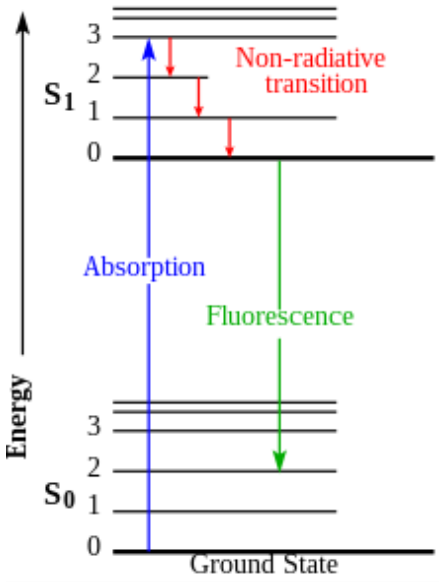

Figure 15 – Jablonski diagram of fluorescence

The excited state S_1 can relax by other mechanisms not involving the emission of a photon. These non-radiative processes compete with fluorescence, decreasing its efficiency. Examples include internal conversion, energy transfer to other molecules and intersystem crossing.[xxxi]

The efficiency of the fluorescence process is described by the quantum yield. This is the ratio between the number of photons emitted by the material to the number of photons absorbed, which refers to the proportion of excited states that result in fluorescence.[xxx]

$$\phi = \frac{Number\ of\ photons\ emitted}{Number\ of\ photons\ absorbed} \quad (4)$$

Fluorescence is exhibited only by certain molecules according to the energy and environment of their bonding electrons. The properties of molecules that influence their fluorescent behaviour are discussed in the following section.

Unlike atomic orbitals in single atoms, the energy states in molecules depend on the nature of the bonds between the atoms in the molecule. In a molecule, covalent bonds between atoms are formed as a result of overlapping atomic orbitals. When these orbitals overlap, they combine to form two molecular orbitals belonging to the pair of atoms, one with higher energy and one with lower energy than the initial atomic orbitals.[xxxiii] The lower energy molecular orbital is called the bonding orbital and can be considered as a region of constructive interference between the two atomic wavefunctions in which electrons are most likely to be found in their ground state. This bonding orbital is more stable and promotes the bonding of the two atoms when occupied. The

higher energy orbital is called the antibonding orbital and can be considered as a region of destructive interference between the two atomic wavefunctions in which electrons are least likely to be found in their ground state. The antibonding orbital is less stable and opposes bonding if occupied.[xxxiv] These molecular orbitals can be represented on an energy level diagram (Figure 16) the simple example of a hydrogen molecule. This shows how the atomic s-orbitals of the two hydrogen atoms combine to form two sigma molecular orbitals, one bonding and one antibonding. In the ground state, both electrons occupy the bonding orbital, creating a stable molecule of H_2.

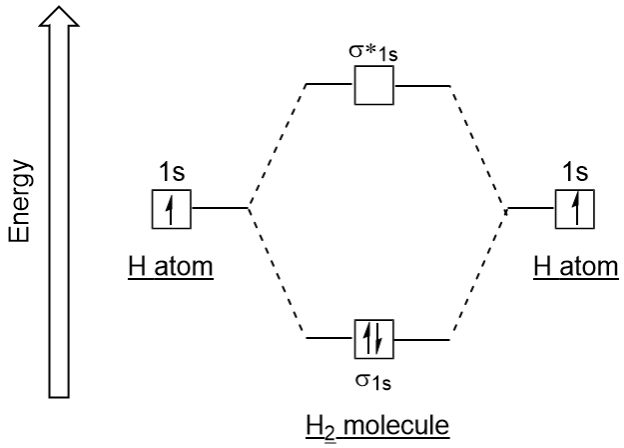

Figure 16 – Molecular orbitals in a hydrogen molecule

An electron must gain energy for fluorescence to occur. As a result, fluorescence occurs most commonly in compounds with a small difference in energy between the ground and excited states because the electron can be promoted more readily.

In most simple molecules consisting of distinct sigma and/or pi bonds, the possible electronic transitions between bonding molecular orbitals all involve large energies, corresponding to very low wavelengths not visible to the human eye. Furthermore, these energies are often large enough to rupture some of the bonds in the molecule, resulting in deactivation of the excited state through dissociation or predissociation without the release of electromagnetic radiation.[xxx] For fluorescence to be observed in the visible range, molecules must have much lower energy differences, such as those containing extensive conjugation within their structures.

The most common examples of such conjugated systems are those consisting of alternating double and single bonds. In these molecules, the delocalisation of pi electrons across the entire conjugated system causes the energy difference between pi bonding molecular orbitals and pi antibonding molecular orbitals to decrease, allowing electrons to be promoted to antibonding orbitals by lower energy radiation.[xxxv]

Example 1: Optical Brightening Agents

Optical brightening agents (OBAs) are chemicals that give a 'whitening' effect to materials such as paper and fabric, enhancing their appearances.[xxxvi] These compounds absorb electromagnetic radiation in the ultraviolet range and emit in the visible blue range. This compensates for the lack of blue light emitted by materials with a more yellow appearance, causing these materials to appear whiter. [xxxvii] Any surface treated with an OBA also emits more visible light than non-fluorescent materials, increasing its apparent brightness.

Figure 17 illustrates the results obtained through fluorescence spectroscopy carried out on a sheet of plain paper illuminated by ultraviolet light. The red line shows the spectrum of the ultraviolet source used for excitation, and the blue line shows the resulting emission spectrum from the paper. The difference between these spectra is shown in the lower plot, demonstrating that some of the shorter wavelength light from the ultraviolet source is absorbed (360 to 400nm), and re-emitted at longer wavelengths (430 to 540nm). The additional emission peak is centred at approximately 480nm, which is in the visible blue region of the electromagnetic spectrum.

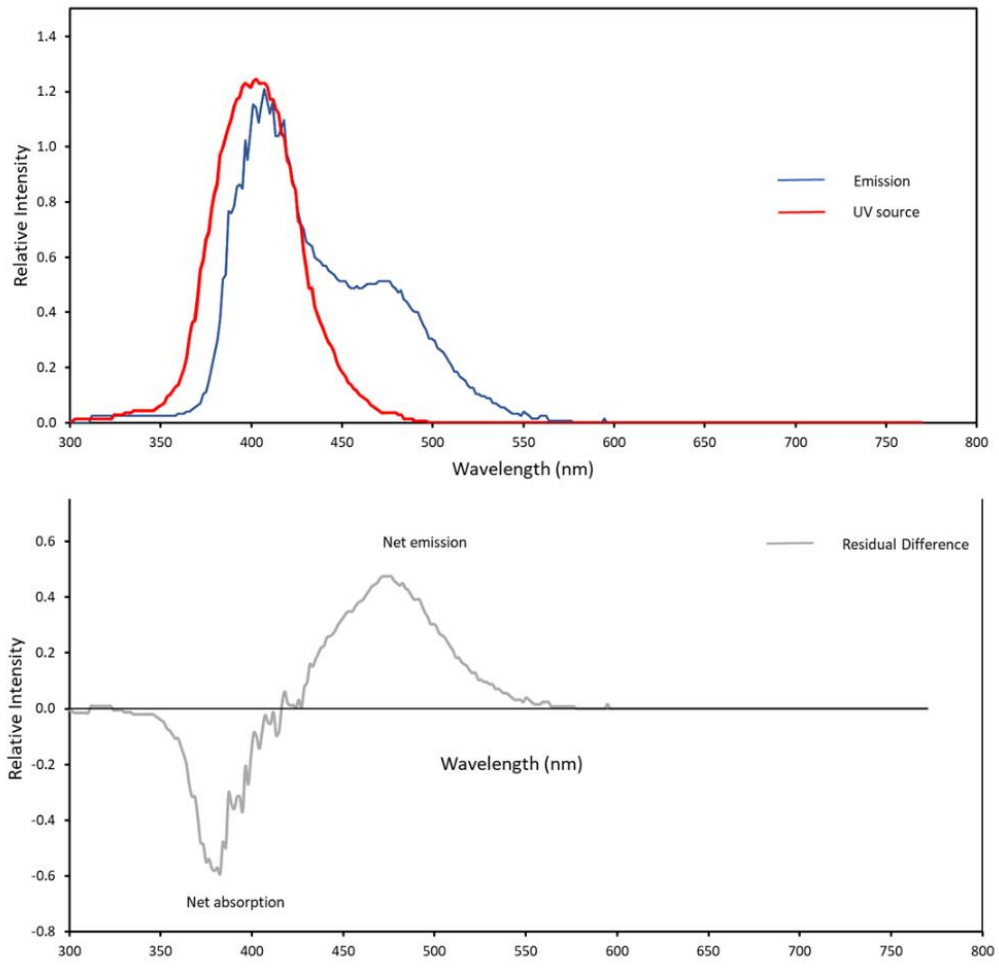

Figure 17 – Emission spectra of paper (blue), ultraviolet source (red) used for excitation and the residual difference (grey)

The most popular examples of optical brightening agents are members of the stilbenes[xxxviii], such as 4,4-diaminostilbene-2,2-disulfonic acid as illustrated in Figure 18.[xxxix]

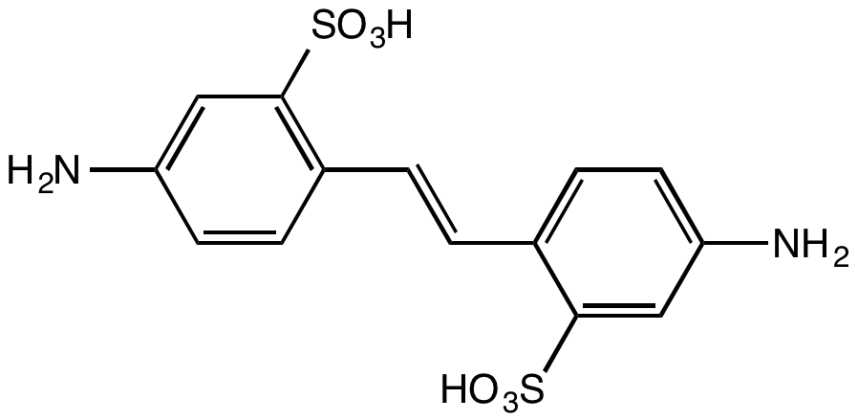

Figure 18 - Structure of 4,4-diaminostilbene-2,2-disulfonic acid

This structure contains extensive conjugation and two aromatic rings, both of which contribute to the delocalisation of electrons across the whole system. As a result, the minimum energy gap is relatively low, allowing these molecules to visibly fluoresce by absorbing in the ultraviolet range and emitting in the visible range.

Example 2: Chemical dyes

Fluorescent molecules are also commonly used as chemical dyes and markers for microscopy and imaging purposes.[xxix] A common example is fluorescein which is used as a contrast agent for diagnostic purposes, bioimaging and as a stain for microscopy.[xl] Its structure is illustrated below in Figure 19.[xli]

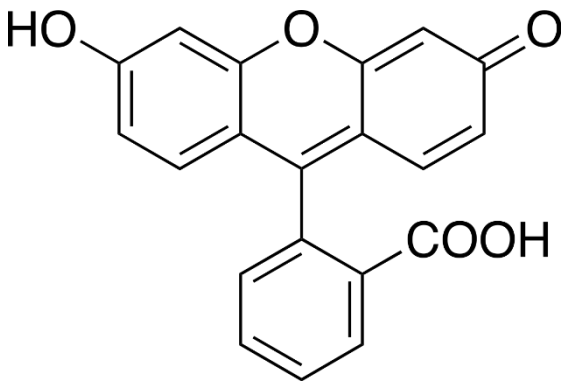

Figure 19 - Structure of fluorescein

Similarly to the molecules used as OBAs described above, fluorescein has a highly conjugated structure including two aromatic rings, allowing it to absorb in the ultraviolet range and emit in the visible green region of the electromagnetic spectrum.

Figure 20 illustrates the results obtained through transmission fluorescence spectroscopy of fluorescein. The graphs show that a broad range of wavelengths from the ultraviolet source are absorbed, and re-emitted as a separate broad emission peak with a maximum of approximately 530nm which is in the green region of the visible electromagnetic spectrum.

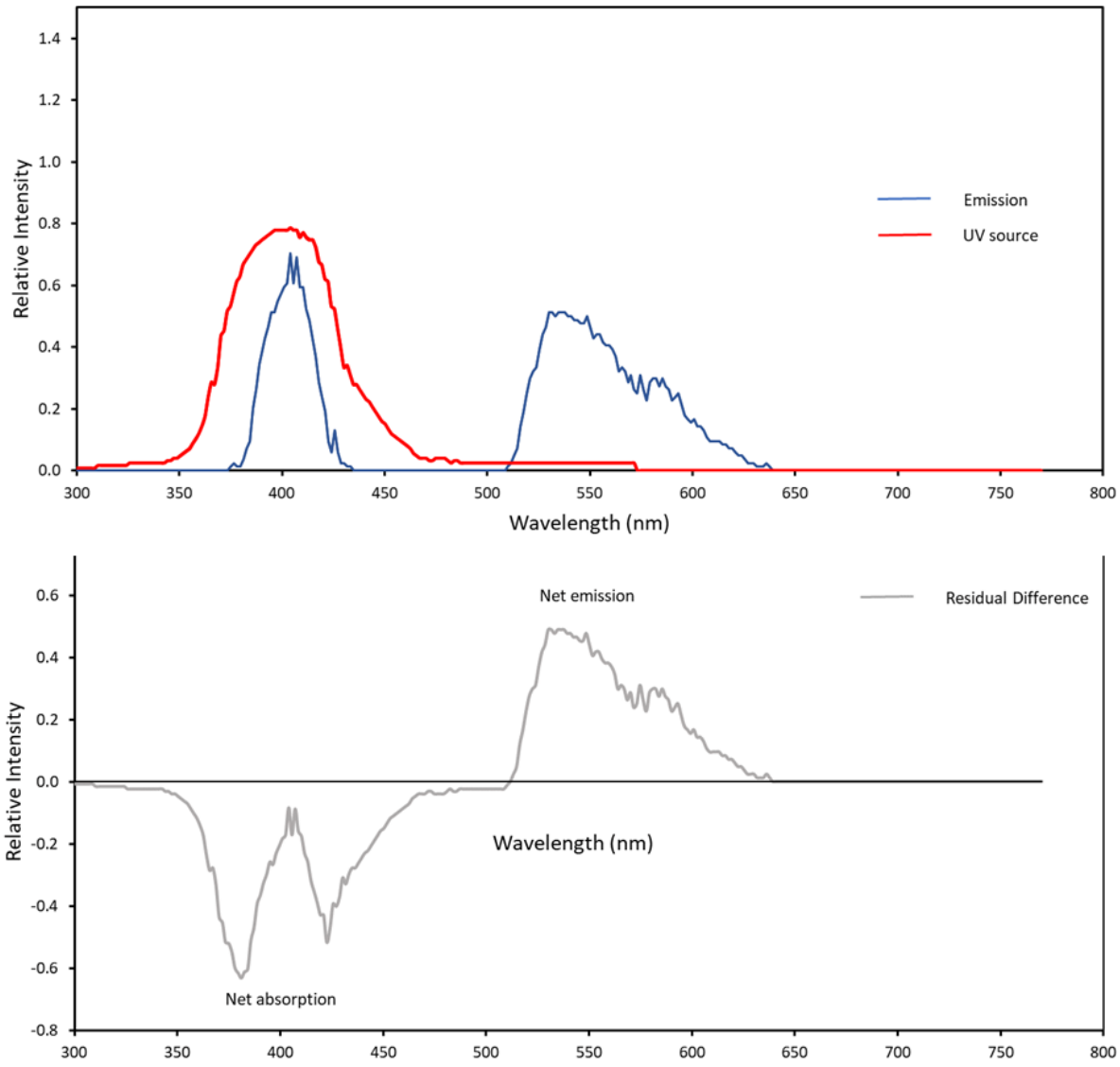

Figure 20 - Emission spectra of fluorescein (blue), ultraviolet source (red) used for excitation and residual difference (grey)

Investigation 4: Quantum dots

Quantum dots are semiconductor nanocrystals that have unique electronic and optical properties that are dependent on their shape and size.[xlii] Quantum dots have regular structures with typical diameters of a few nanometres and are composed of semiconductors such as the elements carbon, silicon or germanium, or from compounds such as CdSe or CdS. Their potential uses include biomarkers and TV screens due to their high photostability, brightness, extinction coefficient and Stokes shift, especially in comparison to chemical dyes such as fluorescein.[xliii] Another major advantage of quantum dots is their size-dependent emission wavelengths, which allows them to be tuned to emit specific colours of light.[xliv] In this section we will be using quantum dots as a model for a simple quantum mechanical system by exploring their optical properties.

As with normal semiconductors, quantum dots have a band gap which is the energy required to promote an electron from the valence band to the conduction band to create a charge carrier. However, because quantum dots have dimensions on the scale of nanometres (on a similar scale to the Bohr radius of their charge carriers) they exhibit quantum confinement of their charge carriers, giving rise to their unique optical and electronic properties. This confinement gives quantum dots bound and discrete energy levels, unlike bulk semiconductors which have continuous energy levels within bands as illustrated in Figure 21. [xlv] These energy levels in quantum dots closely resemble those in naturally occurring atoms and molecules, giving rise to the alternative name 'Artificial Atoms'.[xlvi,xlvii] Quantum dots also have electronic wave functions which closely resemble those in atoms.[xlviii]

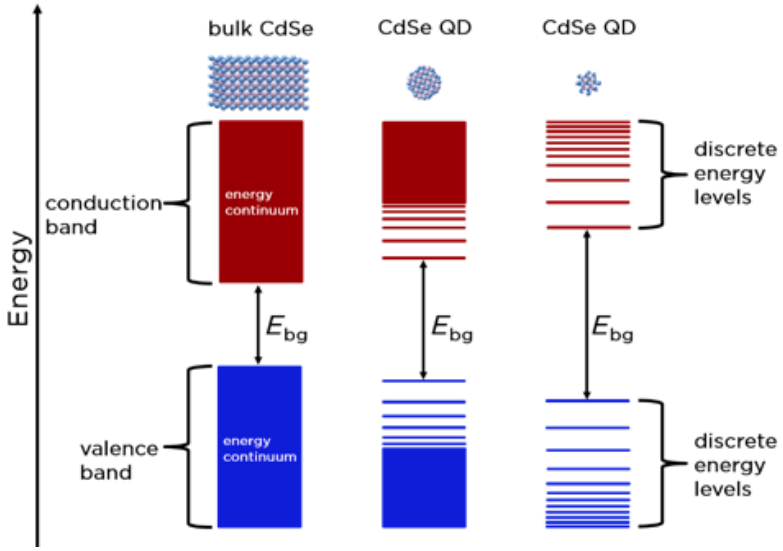

Figure 21 - Band gap and energy levels in quantum dots compared to bulk semiconductors

Particle in a Box model

The behaviour and confinement energy of an electron confined within in a quantum dot can be approximated by the particle in a box model.[xlix]

In quantum mechanics, the particle in a box model describes the movement of a particle in a small area with impenetrable barriers (such as an electron confined within a quantum dot). In contrast to classical systems in which a particle inside a container may move at any speed and is equally likely to be found in any space in the box at any time, the particle in a box model describes how at very small scales of box dimensions (on a similar scale to the de Bohr radius of the particle) the particle may only occupy certain discrete energy levels. Unlike in classical systems, the particle's position probability is also not distributed equally within the container, and it is more likely to be found at certain positions than others according to its energy state. The position of a particle inside the box is described by its wavefunction, ψ, and its probability density of being in a given position is given by the squared modulus of this wavefunction, $|\psi|^2$.

The simplest example of the particle in a box model refers to a one-dimensional system. The particle can move freely in a straight line between two points ($x = 0$, $x = L$), with impenetrable barriers at each of these points. The area between $x = 0$ and $x = L$ can be considered to be a well with zero potential energy and the barriers as regions of space with infinite potential energy. This system is illustrated in Figure 22.

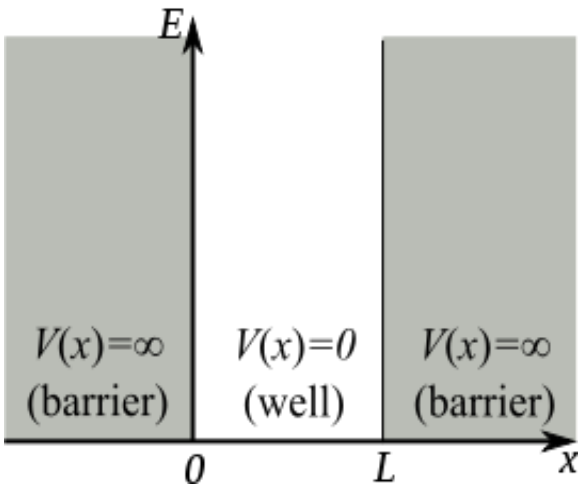

Figure 22 – Illustration of the 1D particle in a box system

The potential energy in this model is dependent on the position of the particle x, as given by

$$V(x) = \begin{cases} 0, 0 < x < L \\ \infty, otherwise \end{cases}$$

5

Since the particle is not acted on by any external forces when inside the box, the wavefunction of this particle inside the box is the same as that of a free particle.

The time-independent Schrödinger equation[i] for a particle moving in one dimension is

$$-\frac{\hbar^2}{2m}\frac{d^2\psi(x)}{dx^2} + V(x)\psi(x) = E\psi(x)$$

6

with

- m the mass of the particle
- x the position of the particle
- E the energy of the particle
- $\hbar$ the reduced Planck Constant $\left(\hbar = \frac{h}{2\pi}\right)$
- ψ(x) the wavefunction of the particle
- V(x) the potential energy of the system

Since the area in which the particle is free to move has zero potential energy ($V = 0$ at all points), this equation can be rewritten as

$$-\frac{\hbar^2}{2m}\frac{d^2\psi(x)}{dx^2} = E\psi(x)$$

7

which has the general solution of

$$\psi(x) = A\,sin\,(kx) + B\,cos\,(kx)$$

8

where A, B, k are all constants.

In order to find the specific solution for this system, the boundary conditions are applied (Appendix B).

This results in a normalised wavefunction for a particle in a 1-dimensional box.

$$\psi = \left(\frac{2}{L}\right)^{\frac{1}{2}} sin\left(\frac{n\pi}{L}x\right)$$

9

This also allows the determination of the possible energies of a particle in a 1-dimensional box.

$$E_n = \frac{n^2\hbar^2\pi^2}{2mL^2} = \frac{n^2h^2}{8mL^2}$$

10

where n is a positive integer.

These results can be illustrated using a ladder diagram as shown in Figure 23.

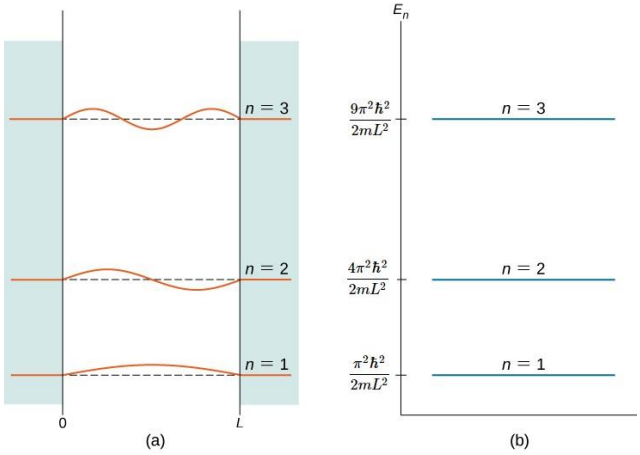

Figure 23 – Energy levels of a particle in a box

This result is significant since it demonstrates that the energy of the particle is quantized and that it has a lowest possible energy, known as the zero-point energy, which is above zero and is given by

$$E_1 = \frac{h^2}{8mL^2}$$

11

This idea that a free-moving particle always has positive energy and can never be at rest contrasts with classical systems in which a particle can be at rest with zero kinetic energy. This theory is also consistent with the Heisenberg Uncertainty Principle which states that

$$\Delta p \Delta x \geq \frac{\hbar}{2}$$

12

We can use this simple particle in a box model to approximate the behaviour of an electron confined within a quantum dot. Solving the corresponding equation for spatial confinement in three dimensional semiconductors gives an equation which describes the emission energy of spherical quantum dots. [li] The first term is the band gap between the valence band and conduction band of the bulk semiconductor, and the second term is the confinement energy of the charge carrier with respect to the radius of the quantum dot.

$$\Delta E(R) = E_{gap} + \frac{h^2}{8R^2 m^*}$$

13

with

- E_{gap} the band gap of the bulk semiconductor
- R the radius of the quantum dot
- m* the effective mass of the charge carrier

This result is significant since it demonstrates that the energy of electromagnetic radiation emitted by a quantum dot increases as its radius decreases. This property of quantum dots allows them to be tuned to emit specific wavelengths of light, leading to their numerous potential applications in biological imaging and TVs.[lii]

In this project fluorescence spectroscopy was used to investigate a sample of commercially available graphene quantum dots.[liii] As pictured using a transmission electron microscope (TEM) in Figure 24, these are disc-shaped structures which are approximately 5nm in diameter (corresponding to approximately 25 atoms across).

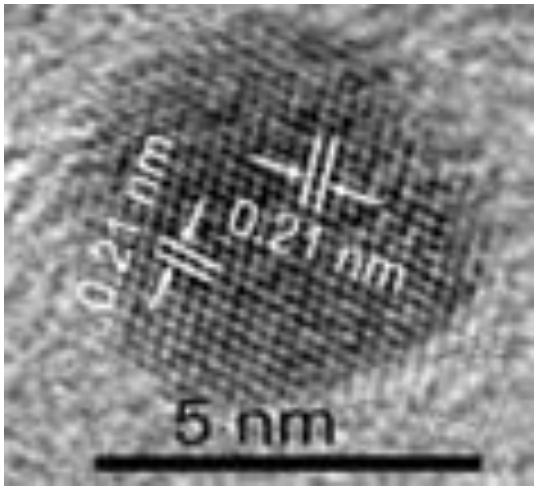

Figure 24 - TEM image of a graphene quantum dot showing the interatomic distance between bonded carbon atoms[liii]

Perpendicular to the plane of the disc the electrons are confined within a distance of approximately 1-2nm, corresponding to several weakly coupled layers of graphene. In the plane of the disc the electrons are confined to a larger space with diameter of approximately 5nm, but they are more mobile and therefore have a much lower effective mass than in the perpendicular direction by a factor many times larger than the difference in length scale. Thus, we expect ground state energies for confinement in the perpendicular direction to be much smaller than for confinement in the plane of the disc, and so we treat these quantum dots as purely two-dimensional systems. For an electron confined in a two-dimensional disc with radius R, it can be shown[liv] that our particle in a box formula can be modified to give the emission energy of graphene quantum dots.[2]

$$\Delta E(R) = E_{gap} + \frac{\hbar^2}{2m^*}\left(\frac{2.4048}{R}\right)^2$$

14

The emission energy of the graphene quantum dots was determined using fluorescence spectroscopy. The quantum dots were suspended in colloidal solution inside a cuvette and illuminated using an ultraviolet flashlight as pictured in Figure 25.

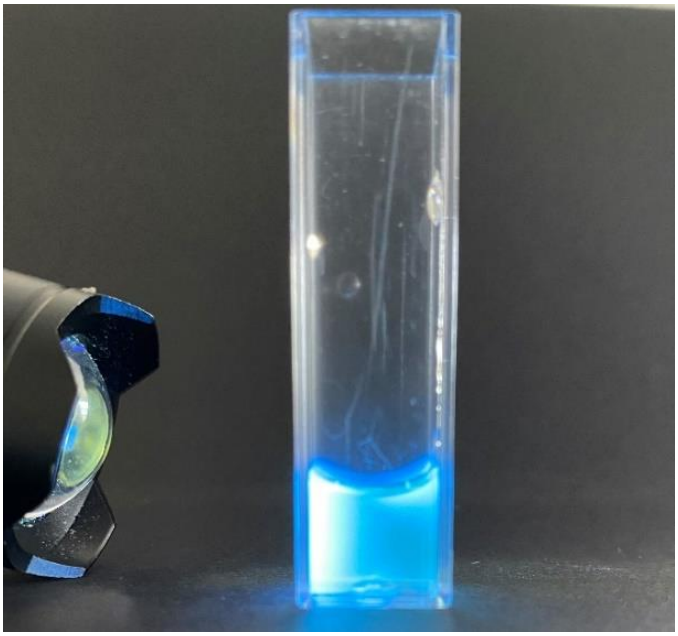

Figure 25 - Illumination of graphene quantum dots in colloidal solution

[2] This system may have additional complexity since an electron promoted to the conduction band leaves behind a hole which is confined in the valence band and has similar quantised energy states to the electron. This additional factor could potentially introduce a factor of two into the equation.

A control experiment performed using the cuvette containing a solution without quantum dots showed no spectral signal.

The results obtained from the sample of quantum dots are illustrated in Figure 26.

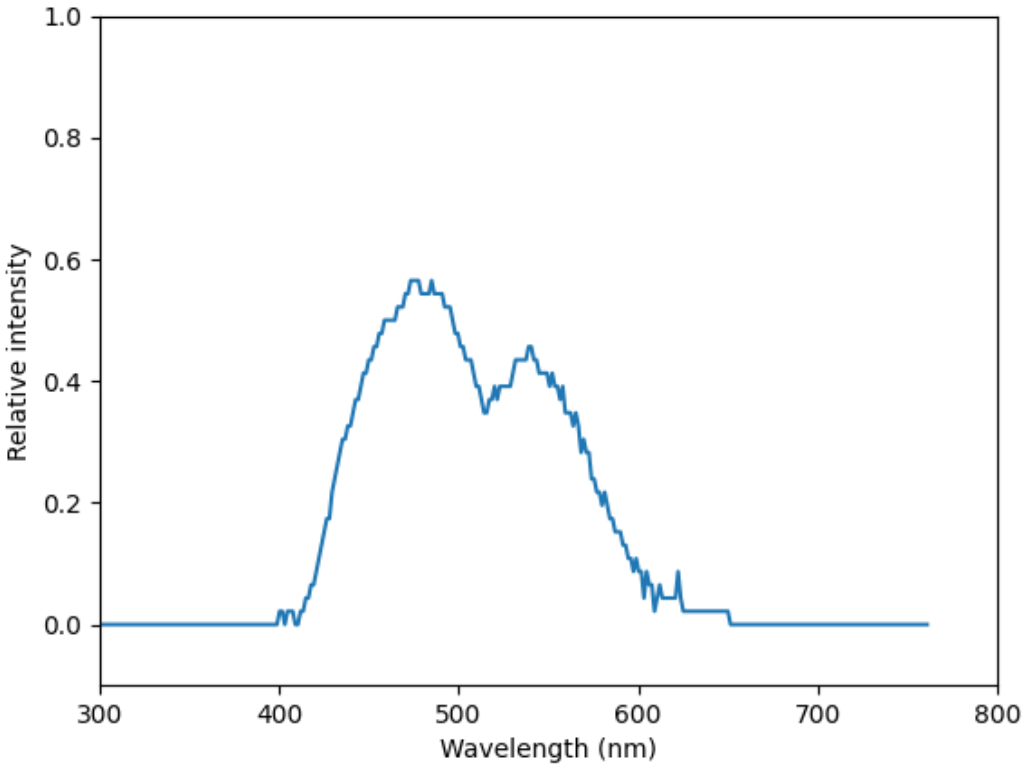

Figure 26 – Spectrum from a colloidal solution of graphene quantum dots

The spectrum contains two peaks with intensity average weighted positions of 480 ± 10nm and 540nm ± 10nm.[3] This is an unexpected result with several plausible explanations:

- There could be two distinct types of quantum dots in the sample, varying in either composition, structure or size.
- The peaks could correspond to different energy level transitions.
- The 480nm peak could be from the quantum dots, and the 540nm peak could be a second order fluorescent effect from the cuvette itself.

Equation 14 can be used to calculate the effective mass of electrons within the graphene quantum dots from these observed emission wavelengths. The band gap of pure bulk graphene is 0eV, although this value may increase with impurities or doping in the structure of the quantum dots. In this model we will consider the band gap to be 0eV.

[3] These errors incorporate uncertainty in the intensity weighted average position and error in the calibration itself.

Assuming a diameter of 5nm, the peak at 480 ± 10nm corresponds to an effective mass of 1.24 ± 0.03 × 10^{-32}kg, and the peak at 540nm ± 10nm corresponds to an effective mass of 1.40 ± 0.03 × 10^{-32}kg. These give an average effective mass[4] of 1.32 ± 0.03 × 10^{-32}kg which is approximately 1.4% of the rest mass of an electron, reasonably consistent with current estimates.

If the presence of the two spectral peaks is instead due to two distinct sizes of disc, the size differential can be calculated using Equation 14. Using the effective mass as 1.4% m_e, the 60nm separation in emission wavelengths corresponds to a difference in diameter between the two discs of approximately 0.3nm. For comparison, the interatomic distance between carbon atoms in these graphene dots is 0.21nm as shown in the TEM image in Figure 24. This suggests that the presence of two spectral peaks could be caused by two sizes of quantum dots with diameters differing by 1 to 2 carbon atoms.

If the two peaks are caused by transitions between different order energy levels within the same size quantum dots, it is likely that the lower energy peak at approximately 540nm corresponds to the transition from n = 1. However, the corresponding n = 2 transition would emit ultraviolet radiation with a wavelength of 220nm, which is outside the detectable range. Alternative possible transitions such as from n = 2 to n = 1 were also considered but none of these were consistent with the data, allowing us to reject this hypothesis.

It is also unlikely that the glass cuvette would fluoresce in the visible spectrum when illuminated by light emitted from the quantum dots, since cuvettes are designed to be neutral holders for such experimentation.

[4] Calculated using the average wavelength of the spectrum as 510 ± 10nm

Conclusion

It has been demonstrated that it is possible to investigate a multitude of light sources and luminescent materials using a simple homemade spectrometer and software in sufficient detail to gain insight into their underlying physical processes. Investigations into filament lamps, LEDs, lasers, elemental discharge lamps, fluorescence in molecular systems and quantum dots were performed. The use of such a spectrometer may be a promising avenue in educational settings.

In particular, the spectrometer was used to derive an estimate for the effective mass of an electron in graphene quantum dots of $1.32 \pm 0.03 \times 10^{-32}$kg which is approximately 1.4% of the rest mass of an electron. This value is reasonably consistent with current estimates.

The presence of dual emission peaks in the spectrum of the sample of quantum dots is a significant finding. Whilst the attribution of the cause is beyond the scope of this project, it is suspected that it arises from two distinct populations of quantum dots in the sample. Should the difference be size alone, this would correspond to a difference in diameter of approximately 0.3nm, which translates to 1 to 2 additional rows of carbon atoms in the lattice. In order to further investigate this hypothesis, the dimensions of the quantum dots in the sample could be determined through independent experimentation, such as through dynamic light scattering or transmission electron microscopy.

Further investigations for the spectrometer could include calibrating the intensity measurements across wavelengths, for example by using a filament lamp of known temperature and the theoretical blackbody curve that its emission spectrum should resemble. This would enable a variety of more profound analyses such as using the spectrometer as a remote thermometer or to determine the composition of samples more accurately. Modifications to the spectrometer itself could include using different diffraction gratings, apertures and lenses in order to improve resolution and sensitivity of the apparatus. With more resources it would also be possible to carry out spectroscopy of multiple samples of quantum dots of known sizes in order to investigate the theoretical relationship between radius and emission wavelength.

References

[i] Brooker, Geoffrey (2003), Modern Classical Optics, Oxford, Oxford University Press

[ii] Newton, Isaac (1705), Opticks: Or A Treatise of the Reflections, Refractions, Inflections and Colours of Light, London, Royal Society

[iii] NASA (2019), Hubble Space Telescope – Space Telescope Imaging Spectrograph. [online] Last accessed 22/5/2022 from https://www.nasa.gov/content/hubble-space-telescope-space-telescope-imaging-spectrograph

[iv] Lakowicz, J.R (2006), Principles of Fluorescence Spectroscopy 3 edn., New York, New York Springer

[v] NASA, Science Mission Doctorate (2010), Visible Light. [online] Last accessed 22/5/2022 from http://science.nasa.gov/ems/09_visiblelight

[vi] Sliney, D (2016), What is light? The visible spectrum and beyond, *Eye* **30**, 222-229

[vii] Geusic, J.E., Marcos, H.M., Van Uitert, L.G. (1964), Laser oscillations in ND-doped yttrium aluminium, yttrium gallium and gadolinium garnets, *Applied Physics Letters* **4** (10): 182

[viii] Astronomy (2019), How do scientists determine the chemical compositions of the planet and stars? [online] Last accessed 22/5/2022 from https://astronomy.com/magazine/ask-astro/2019/06/how-do-scientists-determine-the-chemical-compositions-of-the-planets-and-stars

[ix] Encyclopedia Britannica (1998), D-lines. [online] Last accessed 22/5/2022 from https://www.britannica.com/science/D-lines

[x] NASA, Science and Technology (2000), Spectroscopy Laboratory. [online] Last accessed 22/5/2022 from https://scienceandtechnology.jpl.nasa.gov/spectroscopy-laboratory-0

[xi] Kitchin, C.R. (1995), Optical Astronomical Spectroscopy, Bristol, Institute of Physics Publishing

[xii] David W. (2001), Basics of Spectroscopy, Bellingham, Washington, Society of Photo-Optical Instrumentation Engineers

[xiii] Hearnshaw, J.B. (1986), The analysis of starlight, Cambridge, Cambridge University Press

[xiv] Gregory, Stephen A., Michael Zeilik (1998). Introductory astronomy & astrophysics 4 edn., Fort Worth, Saunders College Publ.

[xv]Biman B. Nath (2013), The Story of Helium and the Birth of Astrophysics, New York, New York Springer

[xvi] Ramsay, William (1895), Helium, a Gaseous Constituent of Certain Minerals Part I, *Proceedings of the Royal Society of London* **58** (347–352), 81–89

[xvii] Gould, R. Gordon (1959), The LASER, Light Amplification by Stimulated Emission of Radiation, University of Michigan, The Ann Arbor Conference on Optical Pumping

[xviii] Britannica Encyclopedia (2021), LED. [online] Last accessed 22/5/2022 from https://www.britannica.com/technology/LED

[xix] Edwards, Kimberly D. (2019), Light Emitting Diodes, University of California at Irvine

[xx] US Department of Energy, Office of Energy Efficiency and Renewable Energy (2017), Solid State Lighting: LED basics. [online] Last accessed 22/5/2022 from https://www.energy.gov/eere/ssl/led-basics

[xxi] Moreno, I., Contreras, U. (2007), Colour distribution from multicolour LED arrays. *Optics Express* **15** (6): 3607–3618

[xxii] US Department of Energy, Office of Energy Efficiency and Renewable Energy (2008), Comparing LEDs to Traditional Light Sources. [online] Last accessed 22/5/2022 from https://web.archive.org/web/20090505080533/http:/www1.eere.energy.gov/buildings/ssl/comparing.html

[xxiii] Britannica Encyclopedia (2021), Incandescent Lamp. [online] Last accessed 22/5/2022 from https://www.britannica.com/technology/incandescent-lamp

[xxiv] Universal Industrial Gases, Inc (2012), Argon (Ar) Properties, Uses, Applications Argon Gas and Liquid Argon. [online] Last accessed 22/5/2022 from https://web.archive.org/web/20120204105153/http:/www.uigi.com/argon.html

[xxv] Encyclopedia Britannica (2021), Blackbody. [online] Last accessed 22/5/2022 from https://www.britannica.com/science/blackbody

[xxvi] Planck, M. (1914), The Theory of Heat Radiation. Translated by Masius, M. (2nd ed.), P. Blakiston's Son & Co.

[xxvii] Encyclopedia Britannica (2017), Fluorescence. [online] Last accessed 22/5/2022 from https://www.britannica.com/science/fluorescence

[xxviii] Smulders, Eduard (2002), Laundry Detergents, Sections 3.4.5 and 10.5.4.4, *Ullmann's Encyclopedia of Industrial Chemistry*, Weinheim, Wiley-VCH

[xxix] Nagano T. (2010), Development of fluorescent probes for bioimaging applications. *Proc Jpn Acad Ser B Phys Biol Sci* **86** (8): 837-47

[xxx] Valeur, Bernard, Berberan-Santos, Mario (2012), Molecular Fluorescence: Principles and Applications, Weinheim, Wiley-VCH

[xxxi] Lakowicz, Joseph R. (1999), Principles of Fluorescence Spectroscopy, New York, Kluwer Academic / Plenum Publishers

[xxxii] Jablonski, Aleksander (1933), Efficiency of Anti-Stokes Fluorescence in Dyes, *Nature* **131**: 839-840

[xxxiii] Atkins, P., de Paula, J. (2006), Atkins Physical Chemistry, Great Britain, Oxford University Press, ISBN: 0-7167-8759-8

[xxxiv] Sannigrahi, A.B., Kar, Tapas (1988), Molecular orbital theory of bond order and valency, *Journal of Chemical Education* **65** (8): 674

[xxxv] Miessler G.L., Tarr D.A. (2013), Inorganic Chemistry 5th edn, Pearson Education

[xxxvi] Hurren, C. (2008), Fabric Testing, Section 9.3.3 (Optical Brightening Agents), Woodhead Publishing

[xxxvii] Smulders, Eduard, Sung, Eric (2002) Laundry Detergents, 2. Ingredients and Products". *Ullmann's Encyclopedia of Industrial Chemistry*, Weinheim, Wiley-VCH

[xxxviii] National Centre for Biotechnology Information (2022), PubChem Compound Summary for CID 5284378, 4,4'-diamino-2,2'-stilbenedisulfonic acid. [online] Last accessed 22/5/2022 from https://pubchem.ncbi.nlm.nih.gov/compound/4_4_-Diamino-2_2_-stilbenedisulfonic-acid

[xxxix] Society of Dyers and Colourists & American Association of Textile Chemists and Colourists (2018), Colour Index. [online] Last accessed 22/5/2022 from https://colour-index.com/

[xl] World Health Organization (2019), World Health Organization model list of essential medicines (21st list), Geneva, World Health Organization

[xli] National Centre for Biotechnology Information (2022), PubChem Compound Summary for CID16850, Fluorescein. [online] Last accessed 22/5/2022 from https://pubchem.ncbi.nlm.nih.gov/compound/Fluorescein

[xlii] Eychmuller, A. (2000), Structure and Photophysics of Semiconductor Nanocrystals, *Journal of Physical Chemistry* **104**(28): 6514-6528

[xliii] Maxwell, T., Santra, S. (2019), Nanoparticles for Biomedical Applications, Elsevier

[xliv] Nguyen H.H (2019), Nano-sized multifunctional Materials, Elsevier

[xlv] Samsung, Insights (2021), What is Quantum Dot display technology? [online] Last accessed 22/5/2022 from https://insights.samsung.com/2021/12/29/what-is-quantum-dot-display-technology/

[xlvi] Ashoori, R. (1996), Electrons in artificial atoms, *Nature* **379**: 413–419

[xlvii] Kastner, M. A. (1993), Artificial Atoms, *Physics Today* **46**(1): 24-31

[xlviii] Benin, U., Cao, Y., Katz, D. *et al.* (1999), Identification of atomic-like electronic states in indium arsenide nanocrystal quantum dots, *Nature* **400**: 542–544

[xlix] Kippeny, T., Swafford, L.A., Rosenthal, S.J. (2002), Semiconductor Nanocrystals: A Powerful Visual Aid for Introducing the Particle in a Box, *Journal of Chemical Education* **79**(9): 1094

[l] Feynman (1996), Lectures on Physics, Volume III, Reading, Massachusetts, Addison-Wesley

[li] Brus, L (1986), Electronic Wave Functions in Semiconductor Clusters: Experiment and Theory, *The Journal of Physical Chemistry* **90**(12): 2555–2560

[lii] Menaka, Jha (2018), Handbook of Nanomaterials for Industrial Applications, Elsevier

[liii] Sigma-Aldrich (2022), Graphene quantum dots. [online] Last accessed 22/5/2022 from https://www.sigmaaldrich.com/GB/en/product/aldrich/900708

[liv] David, C.W. (2006), The Particle in a Box (and in a Circular Box), *Chemistry Education Materials* **12**

Appendices

Appendix A: Image Analysis Software

```
from PIL import Image
import matplotlib.pyplot as plt
import numpy as np

CALIBRATION_CONSTANT = 1.4606 # nm/pixel (old webcam was 1.5366)

def FindMax(xmax, brightness_list, boundary):

    upper = xmax
    while brightness_list[upper] > boundary:
        upper += 1

    lower = xmax
    while brightness_list[lower] > boundary:
        lower -= 1

    sum1 = 0
    sum2 = 0
    for pixel in range(lower, upper + 1):
        sum1 += pixel * brightness_list[pixel]
        sum2 += brightness_list[pixel]

    ans = int(sum1 / sum2)
    return ans

img = Image.open("FILE_PATH", "r")
width, height = img.size

bottom = 0
top = height

pix_val = list(img.getdata())
```

```
brightness_list = []

for col in range(width):

    column = pix_val[col::width]
    red = 0
    green = 0
    blue = 0

    for pixel in column[bottom:top]:
        red += pixel[0]
        green += pixel[1]
        blue += pixel[2]

    red = int(red/height)
    green = int(green/height)
    blue = int(blue/height)

    brightness = (red + green + blue) / len(column)
    brightness_list.append(brightness)

    for i in range(height):
        values[col, i] = (red, green, blue)

ymax = max(brightness_list)
xmax = brightness_list.index(ymax)

xmax = FindMax(xmax, brightness_list, ymax/2)
xarray = list(range(-xmax, width-xmax)) # counts pixels from centre

xarray = [pixel * CALIBRATION_CONSTANT for pixel in xarray]

plt.plot(xarray, brightness_list)
plt.xlabel("Wavelength (nm)")
plt.ylabel("Relative intensity")
plt.show()
```

Appendix B: Boundary conditions

According to the model of the system, the probability that the position of the particle is 0 or L ($x = 0$ or $x = L$) is zero. When $x = 0$, $cos\ (kx) = 1$, so B must equal 0 in order to satisfy our boundary condition. This gives us a wavefunction of

$$\psi(x) = A\ sin\ (kx)$$

In order to compare this with the Schrödinger equation above to solve for k, we must take the second derivative of the wavefunction with respect to x:

$$\frac{d\psi}{dx} = kA\ cos\ (kx)$$

$$\frac{d^2\psi}{dx^2} = -k^2 A\ sin\ (kx) = -k^2\psi$$

Substituting this into the Schrödinger equation above, we can solve for k to get that

$$k = \left(\frac{2mE}{\hbar^2}\right)^{\frac{1}{2}}$$

and so using our above wavefunction,

$$\psi = A\ sin\ (x(\frac{2mE}{\hbar^2})^{\frac{1}{2}})$$

In order to solve for A we must apply our other boundary condition.

When $x = L$, $\psi = 0$, so

$$0 = A\ sin\ (L(\frac{2mE}{\hbar^2})^{\frac{1}{2}})$$

Since $sin\ (a) = 0$ only when $a = n\pi$, this equation can only be true when

$$L(\frac{2mE}{\hbar^2})^{\frac{1}{2}} = n\pi$$

where n is a positive integer (We note that when n = 0, ψ = 0 at all points inside the box. This cannot be the case since the total probability must be 1 (the particle must be inside the box), and so n = 0 is not a valid case).

Substituting this back into our above wavefunction gives us that

$$\psi = A\, sin\left(\frac{n\pi}{L}x\right)$$

Since the total probability of the particle being at a position between $x = 0$ and $x = L$ is 1 (the particle always remains inside the box), we can normalise the wavefunction to get

$$\int_0^L |\psi|^2\ dx = 1$$

$$A^2 \int_0^L sin^2\left(\frac{n\pi}{L}x\right)\ dx = 1$$

By solving this integral (Appendix B.2), we can determine our normalisation constant

$$A\ = \left(\frac{2}{L}\right)^{\frac{1}{2}}$$

Substituting this into our wavefunction gives our normalised wavefunction for a particle in a 1-dimensional box

$$\psi = \left(\frac{2}{L}\right)^{\frac{1}{2}} sin\left(\frac{n\pi}{L}x\right)$$

Using the necessary energy E of a particle for it to satisfy this wavefunction, we can also solve for the possible energies of a particle in a 1-dimensional box

$$E_n = \frac{n^2\hbar^2\pi^2}{2mL^2} = \frac{n^2h^2}{8mL^2}$$

where n is a positive integer.

Appendix B.2: Step-by-step integration

$$A^2 \int_0^L sin^2\,(\frac{n\pi}{L}x)\,dx = 1$$

$$cos\,(2\theta)\ =\ 1 - 2\,sin^2\,(\theta)$$

$$sin^2\,(\theta) = \frac{1 - cos\,(2\theta)}{2}$$

$$A^2 \int_0^L \frac{1 - cos\left(\frac{2n\pi}{L}x\right)}{2} dx = 1$$

$$\frac{A^2}{2} \int_0^L 1 - cos\left(\frac{2n\pi}{L}x\right) dx = 1$$

$$\frac{A^2}{2}\left[x + \frac{2n\pi}{L} sin\left(\frac{2n\pi}{L}x\right)\right]_0^L = 1$$

$$\left\{\frac{A^2 L}{2} + \frac{2n\pi}{L} sin\,(2n\pi)\right\} - \{0\} = 1$$

since n is an integer, $sin\,(2n\pi) = 0$

$$\frac{A^2 L}{2} = 1$$

$$A = (\frac{2}{L})^{\frac{1}{2}}$$